Thermoregulation of integrated photovoltaic panels with bio-based phase change materials

Vinicius Marson[1], Gabriel Bertacco dos Santos[1], João Batista Campos Silva[1], Elaine Maria Cardoso[1,2]

[1]*Dept. of Mechanical Engineering, São Paulo State University (Unesp)*
Avenida Brasil 56, 15385-007, Ilha Solteira, São Paulo, Brazil
vinicius.marson@unesp.br, gabriel.bertacco@unesp.br, campos.silva@unesp.br
[2]*Dept. of Aeronautical Engineering, São Paulo State University (Unesp)*
Av. Profa. Isette Correa Fontão 505, 13876-750, São João da Boa Vista, São Paulo, Brazil
elaine.cardoso@unesp.br

Abstract. Although photovoltaic (PV) technology has achieved significant advancements in harnessing irradiation to generate electricity, different questions remain open, especially regarding the adverse effects of high temperatures on the PV system. As the temperature of PV panels increases, their energy-conversion efficiency decreases, reducing the overall electricity production. High temperatures also accelerate the degradation of the PV panel, leading to shorter operational lifespans and higher maintenance costs. Hence, reducing the PV panel temperature throughout the day can prevent thermal degradation and increase efficiency. In the present work, we numerically evaluate the thermal behavior of a PV system integrated with a phase change material (PCM). The numerical model uses the Finite Volume Method to solve the conservation equations of mass, momentum, and energy. A 3D transient thermal model incorporating the PCM enthalpy formulation was used to analyze the PV panel temperature. The thermal model considers the energy transfer by conduction, convection, and radiation throughout the day. A mean absolute deviation of 3% was obtained for the PV panel temperature when comparing it with experimental data available in the literature. After the numerical model validation, the PCM was changed to a bio-based PCM (bioPCM) consisting of lauric acid, whose melting point is relatively high (43.5 °C), allowing its use in regions of high solar incidence. Furthermore, it has a high latent heat of fusion, being a chemically stable and non-toxic material. Using the proposed bioPCM, a temperature reduction of 7.9°C was obtained, increasing the energy production, on average, by 9% compared to a conventional PV without PCM. Overall, using the proposed bioPCM can avoid excessive losses of energy-conversion efficiency under high irradiance conditions and extend the lifespan of photovoltaic panels.

Keywords: bioPCM, Photovoltaic panel, Thermoregulation

1 Introduction

Recently, the pursuit of renewable energy sources has become a global priority, driven by increasing awareness of the negative impacts of traditional energy sources like oil and coal on the environment and climate. Environmental disasters and alarming signs of climate change underscore the need to transition to cleaner and more sustainable energy generation systems. In this context, solar energy has emerged as one of the most promising solutions to address the energy challenges of the 21st century. Photovoltaic energy, in particular, captures solar radiation to generate electricity directly and cleanly without emitting harmful greenhouse gases or atmospheric pollutants. Moreover, technological advancements and decreasing production costs have made photovoltaic systems increasingly accessible and efficient. Consequently, the installed capacity of solar energy has grown exponentially, playing a significant role in diversifying the global energy mix and reducing carbon emissions [1].

Despite extensive efforts and resources invested in developing new technologies, the energy conversion efficiency of commercial photovoltaic panels remains low, with a maximum of 22.7% [2]. Therefore, the remaining solar energy is either converted into heat or reflected away. Unfortunately, the efficiency of photovoltaic panels decreases as their temperature rises. Hence, cooling systems are necessary to maintain the electrical energy conversion performance of commercial photovoltaic panels , especially in tropical climates with high solar incidence. In this regard, several heat dissipation methods for photovoltaic panels have been proposed [3], which can be categorized into two major groups: passive and active cooling systems.

Passive cooling systems do not require any kind of external energy, whereas active cooling systems require an external energy source to operate [4, 5]. In the case of active cooling, the energy gained from cooling the panel must exceed the energy consumed for cooling it; otherwise, the active cooling process becomes economically unfeasible [6].

Passive cooling techniques can be further classified into three main categories: air cooling, water cooling, and conductive cooling. Passive cooling techniques can include additional components such as piping, containers, or heat exchangers to facilitate natural convection. Passive heat exchangers effectively reduce the panel temperature, are relatively easy to produce, and offer good cost-effectiveness [6].

It is evident that an active heat exchanger is more successful in reducing the panel temperature than a passive heat exchanger. However, this is no longer the case when it comes to energy gains—i.e., the net energy gain is the thermal energy absorbed by the heat exchanger less the electrical energy it consumes. For this reason, in some cases, it becomes advantageous to adopt a passive cooling method to reduce the panel temperature, leading to greater net energy production.

Passive cooling techniques have increasingly evolved towards more complex systems, such as heat sinks, microchannels, heat exchangers, phase change materials (PCMs), nanofluids, thermoelectric generators, or combinations with other systems. In special, phase change materials can absorb a significant amount of heat over a constant temperature range relative to the phase change, serving also as thermal energy storage and temperature control [7]. As a passive cooling technique, it does not require fluid flow or extra electrical energy. Additionally, PCMs are considered an effective solution to utilizing the remaining thermal energy from renewable sources, such as in the case of photovoltaic panels [8].

In selecting the most appropriate PCM, it is also important to consider the nature of the materials composing the PCM. Unfortunately, in most cases, the materials selected for phase change functions are paraffins, which are petroleum-derived materials. In the context of clean and renewable energy, the cooling mechanisms for photovoltaic modules must come from clean and biodegradable sources.

Bio-based PCM (bioPCM) is a new category of organic PCMs that are obtained from underused raw materials [9] and have appropriate thermophysical properties, such as thermochemical stability, no alteration of properties after multiple subsequent phase change cycles, non-toxicity, and comparable enthalpy of fusion to other PCMs like paraffin. These properties, combined with the fact that these materials are byproducts of the food industry, make them a viable alternative to paraffin-based PCMs.

In this context, it becomes necessary to investigate the feasibility of applying bioPCMs to photovoltaic panels for cooling and utilizing residual thermal energy generated by the solar-to-electric energy conversion process. Altogether, bioPCMs present a great potential to reduce the operating temperature of photovoltaic panels, increasing their energy conversion efficiency.

2 Methodology

In order to numerically investigate the feasibility of using bioPCMs in photovoltaic systems, the experimental study of Yousef et al. [10] was selected as a reference for validating the proposed numerical model. The analysis begins by creating a numerical model to replicate the experimental case. After validating the numerical model, the PCM material is replaced, changing it from the original RT-42 to lauric acid.

2.1 Physical and mathematical models

In order to contextualize the problem, a brief explanation of the experiment conducted by Yousef et al. [10] is provided. The experimental study sought to compare the performance of three photovoltaic modules under the local environmental conditions at Benha, Egypt: one panel was coupled with an RT-42 PCM, a second one was coupled with the same PCM interwoven with an aluminum mesh to increase the thermal conductivity of the system, and the last one was kept unchanged, i.e., without the presence of any external cooling system.

The present study aims to reproduce the experimental results of the panel coupled with the RT-42 PCM. To achieve this, some geometric simplifications were made to minimize the complexity of the numerical domain. The rods and fixtures related to the support of the panel and PCM were disregarded, as well as the presence of the ground and other panels around the PV panel of interest. Additionally, the layers that make up the PV panel were consolidated into a single layer with equivalent properties. Overall, these simplifications are not expected to influence the final result significantly.

The numerical model considers three domains: a fluid domain comprising the air around the PV panel, a solid domain representing the PV panel, and a solid/fluid domain of the PCM. The computational domain of the simulation couples these three domains, in which the governing equations are solved using the Finite Volume

Method.

Figure 1 shows a schematic of the computational domain and the PV/PCM system. The dimensions of the computational domain were based on the recommendations of Franke et al. [11].

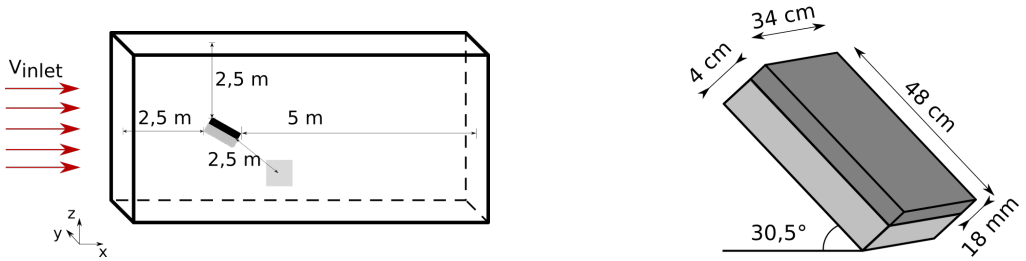

(a) (b)

Figure 1. Dimensions of (a) the computational domain and (b) the PV/PCM system.

Boundary conditions are imposed on the limits of each domain. For the air domain, it was imposed constant uniform velocity profile at the inlet, constant atmospheric pressure at the outlet, and symmetry conditions on the other faces that bound the air domain—i.e., zero spatial derivatives normal to the faces. Perfect thermal contact conditions are imposed at the interfaces between the air, panel, and PCM domains, meaning that the temperature on the adjacent faces of both domains is equal. On the upper face of the panel, a heat generation condition is imposed, representing the solar irradiation less the electrical energy generated by the panel. Figure 2 shows a schematic representation of these boundary conditions.

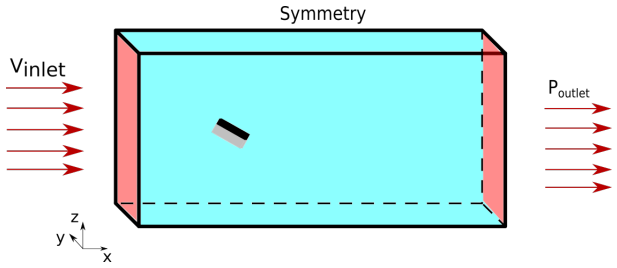

Figure 2. Boundary conditions of the air domain.

It is important to note that some boundary conditions vary during the operation of the PV module. To replicate such behavior, time-dependent boundary conditions were imposed for the ambient temperature and the heat generation on the upper face of the panel. These conditions were interpolated from the 30-minute interval values provided by Yousef et al. [10].

As previously mentioned, the problem was solved using the Finite Volume Method through the established open-source software OpenFOAM®(version 2312, `www.openfoam.com`). OpenFOAM implements the Finite Volume Method with cell-centered variable arrangement to discretize the partial differential equations that describe fluid mechanics.

The `chtMultiRegionFoam` solver was used, which is capable of solving steady-state or transient fluid flow and heat conduction in solids. It handles conjugate heat transfer between regions, buoyancy effects, turbulence, chemical reactions, and radiation. The solution process is segregated, meaning that each variable defining the problem is solved separately and sequentially, and the solution from the preceding equation is used to solve the subsequent ones in an iterative method. The coupling between fluid and solid follows the same strategy: first, the fluid equations are solved using the boundary temperatures obtained from the preceding solid iteration. Then, the solid equations are solved using the boundary temperatures obtained from the preceding fluid iteration. This procedure is repeated until the convergence is reached.

The equations for the two fluid domains are the continuity equation, conservation of momentum, and energy conservation equations, respectively, as

$$\frac{\partial \rho}{\partial t} + \nabla \cdot (\rho \mathbf{v}) = 0, \tag{1}$$

$$\frac{\partial \rho \mathbf{v}}{\partial t} + \nabla \cdot (\rho \mathbf{v}\mathbf{v}) = -\nabla p + \nabla \cdot \left\{ \mu \left[\nabla \mathbf{v} + (\nabla \mathbf{v})^T \right] \right\} + \rho \mathbf{g}, \tag{2}$$

$$\frac{\partial \rho c_p T}{\partial t} + \nabla \cdot [\rho c_p \mathbf{v} T] = \nabla \cdot [k \nabla T] + \dot{q}_V + \rho T \frac{\mathrm{D} c_p}{\mathrm{D} t}, \tag{3}$$

where $\mathbf{v}$ is the velocity vector, ρ is the density, t is the time, p is the pressure, μ is the dynamic viscosity, $\mathbf{g}$ is the gravitational acceleration vector, c_p is the specific heat at constant pressure, T is the temperature, k is the thermal conductivity, and $\dot{q}_V$ is the volumetric heat generation.

For the solid domain, only the energy equation needs to be solved. In this case, the density is constant, the velocity is zero, and since temperature changes are not expressive, the thermal conductivity is considered constant. Thus, the energy equation simplifies to

$$\rho c_p \frac{\partial T}{\partial t} = k\nabla^2 T + \dot{q}_V. \tag{4}$$

For the air region, the following assumptions are adopted: compressible Newtonian fluid, ideal gas, transient regime, and constant properties. The SST k–ω model was selected for modeling turbulence due to its widespread use and robustness for general solutions. For radiation modeling, the *Surface-to-Surface* (S2S) model was used, which focuses solely on the heat exchange between surfaces, i.e., without considering the volumetric domain, only its boundaries.

The `solidificationMeltingSource` function proposed by Swaminathan and Voller [12] is used for modeling the PCM region. In this function, the mushy region—a mixture of liquid and solid—is treated as a porous material of porosity equal to the liquid fraction. Also, momentum dissipation terms are added to the momentum equation to represent the pressure loss caused by the presence of solid material. The interface is a region where the liquid fraction varies from 0 to 1. In this region, the fluid is considered a pseudo-porous material, where the porosity decreases from 1 to 0 as the material solidifies. When the material is fully solidified in a cell, both the porosity and the velocity are zero. In the energy equation, an enthalpy H is considered, which is the sum of the sensible enthalpy h and the latent heat enthalpy ΔH, so that

$$H = h + \Delta H \tag{5}$$

and

$$h = h_{\text{ref}} + \int_{T_{\text{ref}}}^{T} c_p \mathrm{d}T, \tag{6}$$

where h_{ref} represents the enthalpy at a temperature T_{ref} of reference. Lastly, the liquid fraction β is defined as

$$\beta = \begin{cases} 0 & \text{if } T \leq T_s, \\ 1 & \text{if } T \geq T_l, \\ \dfrac{T - T_s}{T_l - T_s} & \text{if } T_s < T < T_l. \end{cases} \tag{7}$$

where T_s is the solidification temperature and T_l is the melting temperature. The melting and solidification temperatures differ because the PCM is not a pure substance.

2.2 Computational Mesh

In the finite volume method, the spatial discretization of the domain, or mesh generation, produces a computational mesh on which the governing equations are solved. Therefore, the quality of the solution depends directly on the quality of the mesh. There are several parameters to measure mesh quality, the most common being non-orthogonality and skewness. These parameters quantify the angle formed between the vector connecting the centers of neighboring cells and the vector normal to their respective faces, and the distance between the vector connecting the centers of neighboring elements to the center of their face. The former is related to both the diffusive and the gradient terms, whereas the latter affects the interpolation of the values at the cell centroid to the cell faces, also influencing diffusive terms, but to a lesser extent compared to non-orthogonality.

The computational mesh was generated using `snappyHexMesh`, an automatic mesh generator within the OpenFOAM ecosystem. `snappyHexMesh` generates predominantly hexahedral meshes in three-dimensional domains. Exceptions to hexahedral elements are typically found near solid boundaries, where polyhedral cells are used to fill spaces between hexahedral cells and the solid geometry. Another exception is in the boundary layer cells, which consist of tetrahedral. Generally, hexahedral cells have superior quality compared to other cell types, resulting in high-quality meshes in most domains when using this methodology. Figure 3 shows a representation of the overall state of the obtained mesh.

In the mesh, tetrahedral elements are present, as mentioned earlier, in the boundary layer. This is necessary to satisfy the recommendation of $y^+ \approx 1$ for the SST k–ω turbulence model. With these mesh refinement modifications, the resulting mesh consists of approximately 1 million elements, 98% of which are hexahedral. The maximum skewness found is 2.5, and the maximum non-orthogonality angle is less than 60°, indicating a high-quality mesh.

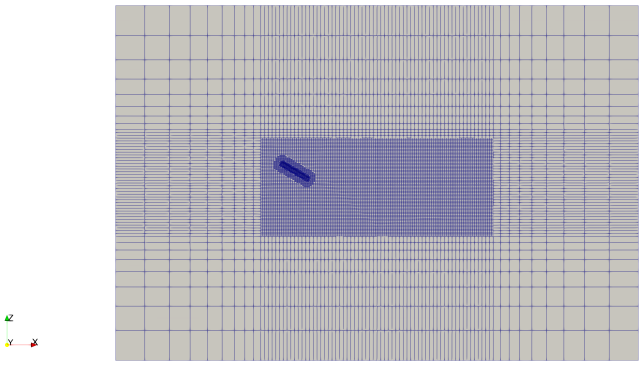

Figure 3. Overall state of the computational mesh.

Additionally, a mesh sensitivity analysis was performed using the Grid Convergence Index (GCI) proposed by Roache [13]. This method allows for measuring of the computational error associated with different mesh sizes using the results of three different mesh solutions. The GCI results are summarized in Table 1. Considering the results of GCI, the error associated with the mesh size is sufficiently low, which justifies choosing the coarser mesh for the subsequent analysis.

Table 1. Grid Convergence Index analysis.

	Mesh 1	**Mesh 2**	**Mesh 3**
Number of cells	4.227.906	2.004.794	949.900
Representative grid size [mm]	46	60	80
Refinement ratio	–	1.30	1.33
Average temperature [°C]	53.16	53.29	53.55
GCI	0.42%	0.74%	1.28%

$r_c = 1.0025$

2.3 PCM selection criteria

As indicated in the literature [14, 15], an appropriate selection of the phase change temperature range for cooling photovoltaic panels is crucial for the overall system performance. Therefore, Hasan et al. [15] proposed a criterion that considers the average nighttime temperatures during summer and the average surface temperatures of the panel during winter days. According to this criterion, the chosen PCM should have a phase change temperature higher than the average nighttime summer temperature and lower than the average panel surface temperature during winter. This ensures that the PCM effectively maintains its intended behavior throughout the year. For the region where Yousef et al. [10] conducted their experiments (Banha, Egypt), the average nighttime summer temperature is 25 °C, and the average panel surface temperature during winter is 45.6 °C. Thus, based on the established selection criterion, the chosen PCM should have a phase change temperature between 25 °C and 45.6 °C.

The paraffinic PCM RT-42 used in the experiments meets the established criteria, as its phase change temperature is 40.5 ºC. In this study, lauric acid, a bioPCM, with a phase change temperature of 43.5 °C was chosen to replace the paraffinic PCM RT-42, a fossil-fuel-based one. Table 2 shows the main thermophysical properties of both PCMs.

As observed in Table 2, the selected bioPCM is relatively similar in terms of thermophysical properties to the RT-42 used in the original experiment. The primary difference lies in their respective origins; while RT-42 is derived from petroleum, lauric acid is a byproduct of the food industry and is found in vegetable oils. Additionally, lauric acid is chemically stable and non-toxic.

Table 2. Thermophysical properties of the RT-42 [10] and the lauric acid [16].

Properties	**RT-42**	**Lauric acid**
Melting temperature [°C]	40.5	43.5
Density [kg/m^3]	880	940
Specific heat capacity [kJ/kg·K]	2.00	1.95
Thermal conductivity [W/m·K]	0.2	0.45
Viscosity [kg/m·s]	0.0235	0.006
Thermal expansion rate [K^{-1}]	$5{\cdot}10^{-4}$	$9{\cdot}10^{-4}$
Latent heat [kJ/kg]	165.0	187.2

3 Results and discussion

Figure 4 compares the average temperature of the PV panel coupled with the RT-42 PCM obtained the mathematical model (T_{sim}) and by the experimental work (T_{exp}) of Yousef et al. [10]. For this comparison, the weather conditions in Benha, Egypt, on July 19, 2020 were considered. The mean absolute percentage deviation between the average panel temperature given by the numerical model and the experimental data was 2.78%, with the highest deviation being 5.03% at 8:30 AM. The results agree with the experimental data, successfully validating the numerical model.

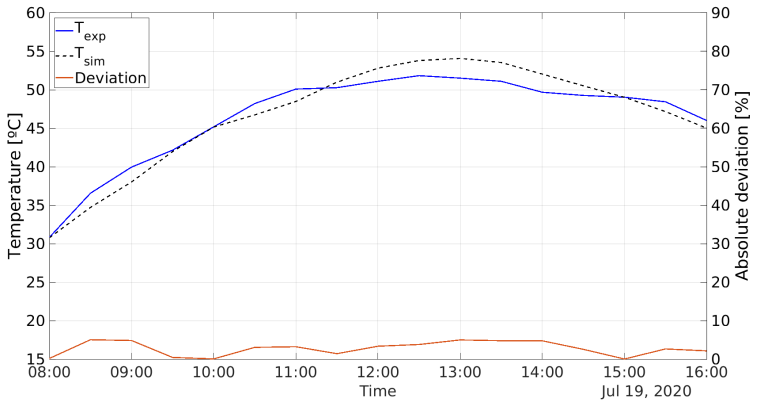

Figure 4. Average temperatures on the photovoltaic panel and mean absolute deviation throughout the day.

Subsequently, the RT-42 PCM was replaced with the lauric acid bioPCM. Figure 5 shows the average temperatures of the panel without any cooling system obtained experimentally by [10] ($T_{PV\ exp}$), the temperatures of the PV panel coupled with the paraffin-based RT-42 PCM ($T_{\text{RT-42 sim}}$), and the lauric acid bioPCM ($T_{\text{Lauric acid sim}}$) obtained through the proposed numerical model.

As shown in Figure 5, the average temperature of the two cooled panels ($T_{\text{RT-42 sim}}$ and $T_{\text{Lauric acid sim}}$) is significantly lower than that of a naturally cooled PV module. Further, the PV/bioPCM system presents a lower average temperature than the PV/RT-42 system at peak solar irradiance. Throughout the day, the reference PV system reaches a maximum temperature of 61 °C, whereas the PV/RT-42 and the PV/bioPCM systems reach a maximum temperature of 54.1 °C and 53.1 °C, respectively, representing a temperature drop of 11.3% and 13.0%. Additionally, according to [10], this reduction in temperature should lead to an approximately 9% increase in power output. This demonstrates that the selected bioPCM can replace the paraffin-based PCM and provide a slightly better thermal performance.

4 Conclusions

In this study, a numerical model was developed to predict the temperature of a commercial photovoltaic module integrated with a phase change material (PCM) from local climatic conditions, such as wind speed, ambient

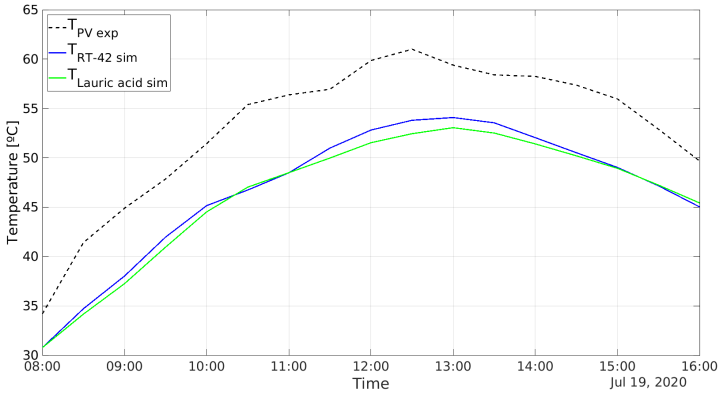

Figure 5. Average temperatures on the PV panel surface throughout the day for the three systems: the PV panel without any cooling mechanism ($T_{\text{PV exp}}$), the one coupled with the RT-42 PCM ($T_{\text{RT-42 sim}}$), and the one coupled with lauric acid bioPCM ($T_{\text{Lauric acid sim}}$).

temperature, and solar irradiance. The model was validated by comparing the numerical results with experimental data available in the literature, showing an average absolute deviation of 2.86% was found. After validation, the numerical model was used to investigate the feasibility of using bioPCMs in photovoltaic systems. Under the analyzed environmental conditions, the data show that the lauric acid bioPCM exhibited better thermal performance than the paraffin-based RT-42 PCM, with a temperature reduction of 15.5% at peak solar irradiance. Therefore, bioPCMs may be used in place of fossil-fuel-based PCMs to reduce the average temperature of PV panels. This result highlights that a simple change of PCM can help reduce the carbon footprint of PV panels, providing a cleaner alternative to paraffin-based PCMs.

Acknowledgements. The authors acknowledge the National Laboratory for Scientific Computing (LNCC/MCTI, Brazil) for providing the HPC resources of the SDumont supercomputer (`http://sdumont.lncc.br`), which have greatly contributed to the research results reported in this study. E.M. Cardoso is grateful for the financial support from Conselho Nacional de Desenvolvimento Científico e Tecnológico (grants number 309848/2020-2 and 305040/2023-5) and Fundação de Amparo à Pesquisa do Estado de São Paulo (grants numbers 2013/15431-7, 2019/02566-8 and 2022/15765-1). V. Marson was financed in part by the Coordenação de Aperfeiçoamento de Pessoal de Nível Superior – Brasil (CAPES) – Finance Code 001.

Authorship statement. The authors are the only ones responsible for the printed material included in this paper.

References

[1] BEN. Balanço energético nacional. `https://www.epe.gov.br/sites-pt/publicacoes-dados-abertos/publicacoes/PublicacoesArquivos/publicacao-675/topico-638/BEN2022.pdf`, 2022.

[2] C. T. Machado and F. S. Miranda. Energia solar fotovoltaica: Uma breve revisão. *Revista virtual de química*, vol. 7, pp. 1–18, 2015.

[3] S. S. Koohestani, S. Nižetić, and M. Santamouris. Comparative review and evaluation of state-of-the-art photovoltaic cooling technologies. *Journal of Cleaner Production*, vol. 406, pp. 136953–136953, 2023.

[4] H. Teo, P. Lee, and M. Hawlader. An active cooling system for photovoltaic modules. *Applied Energy*, vol. 90, n. 1, pp. 309–315. Energy Solutions for a Sustainable World, Special Issue of International Conference of Applied Energy, ICA2010, April 21-23, 2010, Singapore, 2012.

[5] S. Wu and C. Xiong. Passive cooling technology for photovoltaic panels for domestic houses. *International Journal of Low-Carbon Technologies*, vol. 9, n. 2, pp. 118–126, 2014.

[6] P. Dwivedi, K. Sudhakar, A. Soni, E. Solomin, and I. Kirpichnikova. Advanced cooling techniques of PV modules: A state of art. *Case Studies in Thermal Engineering*, vol. 21, pp. 100674, 2020.

[7] T. Ma, Z. Li, and J. Zhao. Photovoltaic panel integrated with phase change materials (PV-PCM): technology overview and materials selection. *Renewable and Sustainable Energy Reviews*, vol. 116, pp. 109406, 2019.

[8] A. Pandey, M. Hossain, V. Tyagi, N. Abd Rahim, J. A. Selvaraj, and A. Sari. Novel approaches and recent developments on potential applications of phase change materials in solar energy. *Renewable and Sustainable*

Energy Reviews, vol. 82, pp. 281–323, 2018.
[9] R. Sharma, P. Ganesan, V. Tyagi, H. Metselaar, and S. Sandaran. Developments in organic solid–liquid phase change materials and their applications in thermal energy storage. *Energy Conversion and Management*, vol. 95, pp. 193–228, 2015.
[10] M. S. Yousef, M. Sharaf, and A. Huzayyin. Energy, exergy, economic, and enviroeconomic assessment of a photovoltaic module incorporated with a paraffin-metal foam composite: An experimental study. *Energy*, vol. 238, pp. 121807, 2022.
[11] J. Franke, A. Hellsten, H. Schlünzen, and B. Carissimo. Best practice guideline for cfd simulation of flows in the urban environment. *International Journal of Environment and Pollution*, vol. 44, pp. 419–427, 2011.
[12] C. Swaminathan and V. Voller. A general enthalpy method for modeling solidification processes. *Metallurgical Transactions B*, vol. 23, pp. 651–664, 1992.
[13] P. J. Roache. Perspective: A method for uniform reporting of grid refinement studies. *Journal of Fluids Engineering*, vol. 116, pp. 405–413, 1994.
[14] N. Savvakis and T. Tsoutsos. Theoretical design and experimental evaluation of a PV+PCM system in the mediterranean climate. *Energy*, vol. 220, pp. 119690, 2021.
[15] A. Hasan, J. Sarwar, H. Alnoman, and S. Abdelbaqi. Yearly energy performance of a photovoltaic-phase change material (PV-PCM) system in hot climate. *Solar Energy*, vol. 146, pp. 417–429, 2017.
[16] D. G. Peña, I. A. deMiguel, M. D. Mediavilla, and C. A. Tristán. Experimental analysis of a novel PV/T panel with PCM and heat pipes. *Sustainability*, vol. 12, n. 5, 2020.